

Direct Visualization of Quasi-Liquid Layers on Ice Crystal Surfaces Induced by Hydrogen Chloride Gas

Ken Nagashima,* Gen Sazaki, Tetsuya Hama, Harutoshi Asakawa,[†] Ken-ichiro Murata, and Yoshinori Furukawa

Institute of Low Temperature Science, Hokkaido University, N19-W8, Kita-ku, Sapporo 060-0819, Japan

S Supporting Information

ABSTRACT: Surface melting of ice crystals forms quasi-liquid layers (QLLs) on ice surfaces, and affects a wide variety of natural phenomena. Since QLLs enhance various chemical reactions in ice clouds, the formation of QLLs by atmospheric gases has been studied intensively. However, such studies were performed using spectroscopy techniques, which have low spatial resolution. Here we show the first direct visualization of QLLs on ice basal faces in the presence of hydrogen chloride (HCl) gas (model atmospheric gas) by advanced optical microscopy, which can visualize individual 0.37 nm-thick elementary steps on ice crystal surfaces. We found that the HCl gas induced the appearances of QLLs with a droplet shape in the temperature range from -15.0 to -1.5 °C, where no QLL appears in the absence of HCl gas. This result indicates that HCl gas adsorbed on ice crystal surfaces probably changed the surface structure of ice crystals and then induced the subsequent melting of ice surfaces. We also observed the movement, shape change, and splitting of the droplet QLLs when water vapor was undersaturated. The long-term (1 h) existence of the droplet QLLs under the undersaturated conditions strongly suggests that the droplet QLLs were thermodynamically stable HCl solutions.



1. INTRODUCTION

Ice is one of the most abundant crystals on the earth, and hence its phase transitions exert enormous influence on the global environment.¹ Surface melting of ice crystals is one of such phase transitions:^{2,3} ice crystal surfaces are covered with thin liquid layers, so-called quasi-liquid layers (QLLs), even below the melting point (0 °C). It is widely acknowledged that surface melting of ice crystals governs wide variety of natural phenomena, such as shapes of snowflakes, generation of thunder, frost heave, and so on.³ After M. Faraday first proposed the existence of QLLs in 1842,⁴ QLLs on ice crystal surfaces were confirmed by various methods (see Table S1 in the reference⁵). However, the onset temperatures of surface melting and the thickness of QLLs showed considerable variation, depending on both measurement methods and researchers.^{6–8}

Recently, we and Olympus Engineering Co., Ltd. have developed laser confocal microscopy combined with differential interference contrast microscopy (LCM-DIM),^{9,10} by which we succeeded in the direct visualization of 0.37 nm-thick elementary steps and QLLs on ice basal faces for the first time with enough spatial and temporal resolution.^{5,10} Subsequently, the direct observations of QLLs revealed the appearance of two types of QLLs with different morphologies,⁵ the appearance temperatures of QLLs on basal and other high-index faces,^{5,11} the inducement of the formation of QLLs by strain,¹² and the characteristic velocities of QLLs.¹³ The important feature of these studies was the precise calibration of water vapor pressure by measuring the dynamics of individual elementary steps on ice crystal surfaces using

LCM-DIM.¹⁴ Because of high reproducibility guaranteed by the precise calibration, we believe that we can perform the visualization of QLLs in the most reliable way.

We investigated so far the appearance of QLLs in a pure system, although the presence of small amount of impurities plays crucially important roles in a wide variety of natural phenomena.^{3,15} Hence, it is important to investigate the effects of impurities on the formation of QLLs and also on the growth/sublimation of ice crystals. One of such examples is the effect of atmospheric gases on the formation of QLLs.^{16,17} In particular, the effect of hydrogen chloride (HCl) gas has been studied most intensively, since HCl gas plays important roles in ozone-depleting reactions. Polar stratospheric clouds that are composed of many tiny ice crystals are formed at the same altitude of ozone layers in a polar stratospheric. McNeil (2006)¹⁸ found by ellipsometry that HCl gas induces the formation of QLLs on ice crystal surfaces, and found that the presence of QLLs enhances chemical reactions that finally leads to the ozone depletion. As a result, the ozone depletion locally occurs in the polar region. However, such studies were performed using spectroscopy techniques, which do not have enough spatial resolution to reveal the dynamic behavior of individual QLLs. Hence, we conceived that the direct visualization by LCM-DIM would also become a promising means to study the effect of atmospheric gases.

Received: January 11, 2016

Revised: February 12, 2016

Published: February 16, 2016



In this study, we chose HCl gas as model atmospheric gas, and tried to visualize QLLs induced by HCl gas on ice crystal surfaces by LCM-DIM, which has enough spatial and temporal resolution. We investigated the appearance temperature and dynamics of QLLs on ice crystal surfaces in the presence of HCl gas. Then we discussed the differences in the results obtained in the presence and absence of HCl gas.

2. EXPERIMENTAL METHODS

The LCM-DIM system used in this study included all of the improvements reported in our recent study on the observation of elementary steps on ice crystal surfaces.¹⁰ Figure 1 shows a

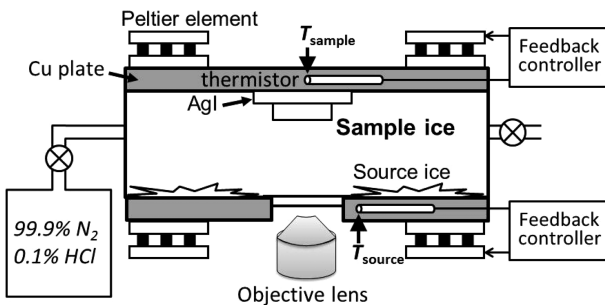


Figure 1. A sectional schematic drawing of an observation chamber. The temperatures of upper and lower Cu plates (T_{sample} and T_{source}) were independently controlled using Peltier elements. Sample ice crystals for the in situ observation were grown on the upper Cu plate. Ambient water vapor pressure of sample ice crystals was controlled by T_{source} . Details of the chamber are shown in Sasaki et al. (2010).¹⁰

cross-sectional schematic illustration of an observation chamber. The chamber had upper and lower Cu plates, whose temperatures T_{sample} and T_{source} were separately controlled using Peltier elements. At the center of the upper Cu plate, a cleaved AgI crystal, known as an ice nucleating agent, was attached using heat grease.

The temperatures of the upper and lower Cu plates were first set at $T_{\text{sample}} = 20.0$ and $T_{\text{source}} = -15.0$ °C, respectively. Water vapor was then supplied to the inside of the chamber by nitrogen gas bubbled through water (flow rate = 500 mL/min). Ice crystals were grown on the lower Cu plate for 1 h: these ice crystals were used as a source of water vapor in the subsequent process. Next, nitrogen gas including 0.1% HCl gas (partial pressure of HCl gas, $P_{\text{HCl}} = 100$ Pa) was injected into the chamber for 5 min (flow rate: 10 mL/min), and then the chamber was kept airtight. Since the volume of the N₂/HCl gas injected was 10 times larger than the inner volume of the chamber, the gas in the chamber was fully replaced with the N₂/HCl gas. During the injection, melting and evaporation of the source ices could be neglected because of the slow flow rate: we confirmed it by another observation experiment. The total pressure was kept at atmospheric pressure using nitrogen gas.

The temperatures of the upper and lower Cu plates were then kept at $T_{\text{sample}} = -15.0$ and $T_{\text{source}} = -13.0$ °C, respectively. Water vapor evaporated from the source ice crystals was supplied to the cleaved AgI crystal. On the AgI crystal, sample ice crystals were grown heteroepitaxially, until the lateral size and height of the sample ice crystals reached several hundred micrometers. Since the total volume of the source ice crystals was significantly larger than that of the sample ice crystals on the AgI crystal, the partial pressure of

water vapor $P_{\text{H}_2\text{O}}$ in the chamber was determined by the equilibrium vapor pressure of the source ice crystals. By separately controlling T_{sample} and T_{source} , the growth temperature of the sample ice crystals and the supersaturation $\sigma = (P_{\text{H}_2\text{O}} - P_e)/P_e$ of the water vapor inside the chamber were adjusted independently (here P_e is the solid–vapor equilibrium pressure). Other details of the chamber, such as the calibration of T_{sample} and the evaluation of supersaturation were reported in our recent study.¹⁴ Circles in Figure 2 show T_{sample} and $P_{\text{H}_2\text{O}}$ examined in this study.

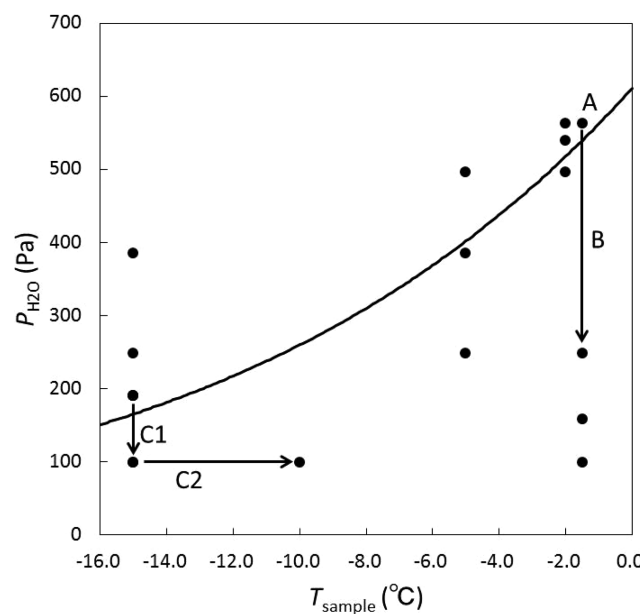


Figure 2. Experimental conditions explored in this study (circles). T_{sample} and $P_{\text{H}_2\text{O}}$ denote the temperature of sample ice crystals and the partial pressure of water vapor, respectively. The solid curve shows the solid–vapor equilibrium curve of water. The circle A, arrow B, and arrows C1 and C2, respectively, show the experimental conditions in Figures 3–5

3. RESULTS AND DISCUSSION

We first observed, by LCM-DIM, a surface morphology of a basal face of an ice crystal that was grown in supersaturated water vapor in the presence of HCl gas. Figure 3A indicates that many hemispherical objects of 10–30 μm in diameter existed on the basal face. In this study, the differential interference contrast was adjusted as if the ice crystal surfaces were illuminated by a light beam slanted from the upper left to the lower right direction, as explained in Figure S1. Hence, the differential interference contrast of a hemispherical object smaller than 15 μm in diameter (marked by a white arrow) demonstrates that the hemispherical object had a convex shape. With increasing diameter of hemispherical objects, height of the objects increased. Hence, when the diameter of a hemispherical object was larger than 15 μm (marked by a black arrow), such a hemispherical object exhibited complex contrast that consisted of both the differential interference contrast and the contrast of interference fringes formed from the outer surface of the hemispherical object and the ice-hemispherical object interface. The height of the 15-μm-diameter hemispherical object is estimated to be about half wavelength (340 nm), although exact

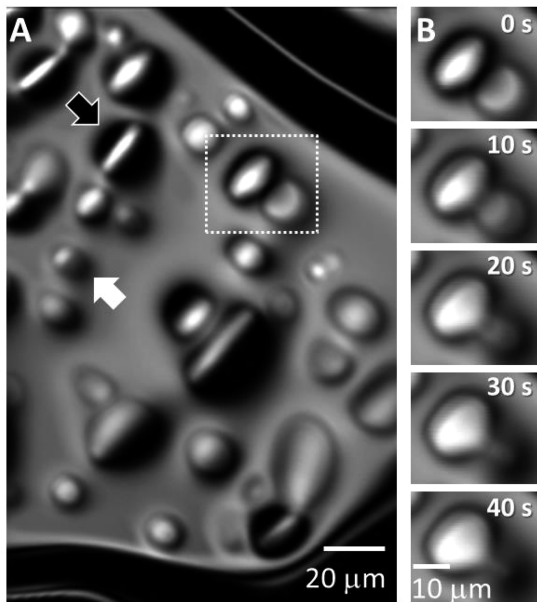


Figure 3. Droplet QLLs formed on an ice basal face grown in the presence of HCl gas. (A) An LCM-DIM image taken in supersaturated water vapor (Figure 2A, $T_{\text{sample}} = -1.5 \text{ }^{\circ}\text{C}$, $P_{\text{HCl}} = 100 \text{ Pa}$, $P_{\text{H}_2\text{O}} = 560 \text{ Pa}$, and $\sigma = 0.1$). (B) Successive images during the coalescence of adjacent liquid layers marked by a white dotted rectangle in A. Differential interference contrasts of droplet QLLs marked by white and black arrows are explained in the main text.

evaluation is difficult. When the diameter of a hemispherical object was larger than $50 \mu\text{m}$, the contrast of such an object was dominated mainly by the contrast of the interference fringes (shown as contour lines, Figure S2).

We could observe the coalescence of adjacent hemispherical objects. Figure 3B shows successive images in the area marked by a white dotted rectangle in Figure 3A. Adjacent hemispherical objects coalesced on a time scale of several tens of seconds. This result indicates that the hemispherical objects displayed fluidity. In addition, we could also observe the movement, shape change, and splitting of hemispherical objects: we will explain later in Figures 4 and 5. Hence, we concluded that the hemispherical object was not a solid phase (ice) but a liquid (QLL) phase that appeared below $0 \text{ }^{\circ}\text{C}$: in this study we defined a QLL as a liquid layer formed below $0 \text{ }^{\circ}\text{C}$.

Figure 4 and Movie S1 show the influences of supersaturation of water vapor on the behavior of droplet QLLs. After the images in Figure 3 were taken, we kept the temperature of the ice basal face constant at $-1.5 \text{ }^{\circ}\text{C}$, and then gradually decreased water vapor pressure from 560 to 250 Pa (Figure 2B). Under supersaturated (Figure 4A) and equilibrium (Figure 4B) conditions, the shape of the droplet QLLs was almost the same as that shown in Figure 3. However, after the water vapor pressure became undersaturated (Figures 4C–F), the shape of the droplet QLLs became unstable (marked by white arrows in Figure 4): a finger-like pattern appeared and then the droplet QLL broke into several smaller droplets.

In Figures 3 and 4, we observed the behavior of droplet QLLs at $-1.5 \text{ }^{\circ}\text{C}$ in supersaturated and undersaturated water vapor in the presence of HCl gas. In contrast, in the absence of HCl gas, we could observe the appearance of QLLs of a droplet type on ice basal faces, only at temperature higher than -1.5

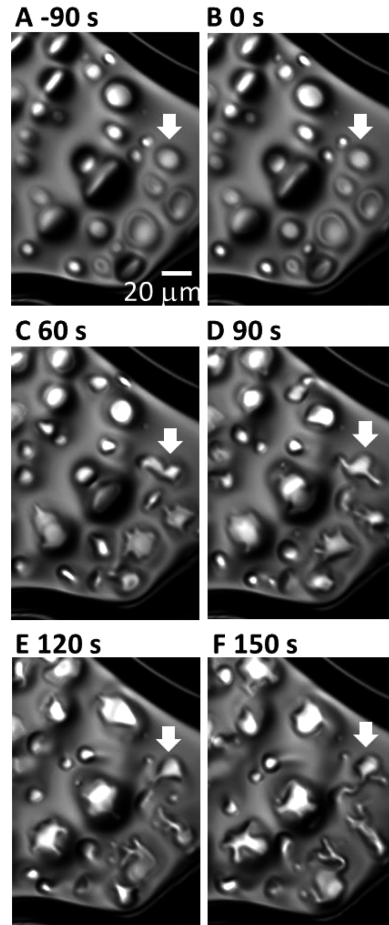


Figure 4. Effects of supersaturation of water vapor on the behavior of droplet QLLs on an ice basal face in the presence of HCl gas. After the images in Figure 3 were taken, we kept the temperature of the ice basal face constant at $-1.5 \text{ }^{\circ}\text{C}$, then we gradually decreased the water vapor pressure from 560 ($\sigma = 0.04$) to 250 Pa ($\sigma = -0.5$). The water vapor was supersaturated (A), equilibrium (B) and undersaturated (C–F). The behavior of the droplet QLLs marked by a white arrow is explained in the main text. A movie of the process from A to F is available as Movie S1.

$\text{ }^{\circ}\text{C}$.⁵ Hence, to examine whether the droplet QLLs observed in this study correspond to the droplet QLLs observed in the absence of HCl gas, we decreased the temperature of ice basal faces to $-15.0 \text{ }^{\circ}\text{C}$, which is the lowest temperature of our observation chamber. Then we performed the similar observation. Figure 5 shows the result.

First, we kept the temperature of an ice basal face constant at $-15.0 \text{ }^{\circ}\text{C}$, and then gradually decreased the water vapor pressure from 190 to 100 Pa (the process C1 in Figure 2). Under supersaturated (Figure 5A) and equilibrium (Figure 5B) conditions, the shape of droplet QLLs did not change, as in the case of Figures 4A and B. However, under undersaturated conditions (Figure 5C and D), the finger-like pattern appeared (marked by black arrows), and then the droplet QLLs gradually split, as in the case of Figure 4C–F.

To increase the degree of undersaturation of the water vapor further, second, we kept the water vapor pressure constant at 100 Pa, then increased the temperature of the ice basal face from $-15.0 \text{ }^{\circ}\text{C}$ to $-10.0 \text{ }^{\circ}\text{C}$ (Figure 5E–H and Movie S2), as marked by C2 in Figure 2. As the degree of undersaturation increased, the movement of the splitting of the droplet QLLs

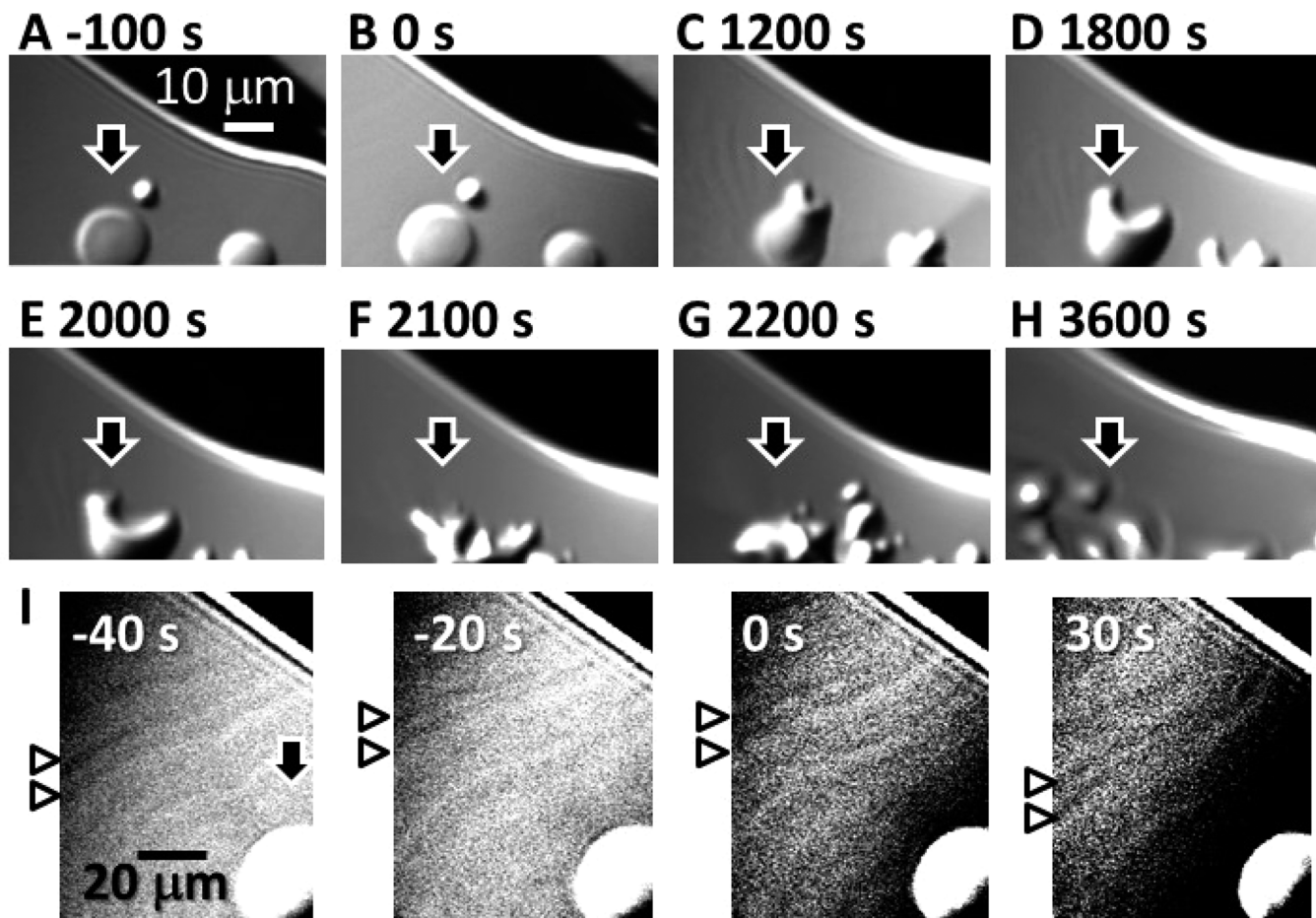


Figure 5. Droplet QLLs on an ice basal face at $-15.0 \sim -10.0$ °C in the presence of HCl gas. First, we kept the temperature of an ice basal face constant at -15.0 °C, then we gradually decreased the water vapor pressure from 190 ($\sigma = 0.2$) to 100 Pa ($\sigma = -0.4$): the water vapor was supersaturated (A), equilibrium (B) and undersaturated (C–D). To increase the degree of undersaturation of the water vapor further, second, we kept the water vapor pressure constant at 100 Pa, then we gradually increased the temperature of the ice basal face from -15.0 to -10.0 °C ($\sigma = -0.6$): the water vapor became further undersaturated (E–H). The behavior of the droplet QLL marked by a black arrow is explained in the main text. A movie of the process from E to G is available as [Movie S2](#). (I) Successive enlarged images around the droplet QLL, marked by the black arrow in A–H. Two white triangles show that elementary steps advanced and receded toward the upper-left and lower-right directions under supersaturated and undersaturated conditions, respectively. The contrast of the images in I was more highly adjusted than those in A–H so that elementary steps became visible.

accelerated. Finally, the droplet QLLs were broke into smaller droplets.

As shown in Figure 5, in the presence of HCl gas, we could observe the droplet QLLs even at -15.0 °C, where no droplet QLL appears in the absence of HCl gas.⁵ In addition, we could observe the droplet QLLs on ice basal faces under a wide variety of conditions summarized in Figure 2. These results clearly indicate that in the presence of HCl gas, the temperature range of the appearances of droplet QLLs is fully different from that in the absence of the gas. Hence, we concluded that the droplet QLLs observed in this study were induced by HCl gas, indicating that HCl gas adsorbed on ice crystal surfaces probably changed the surface structure of ice crystals and then induced the subsequent melting of ice surfaces.

It is natural to assume that HCl gas homogeneously adsorbed on ice crystal surfaces. However, the HCl-induced droplet QLLs did not appear homogeneously but always emerged locally exhibiting a droplet shape, as shown in Figures 3–5. Although we have no experimental evidence, an energy barrier for the nucleation of the HCl-induced QLLs might be relatively high.

As shown in Figures 3 and 4, when many droplet QLLs appeared on ice crystal surfaces, we could not visualize elementary steps on ice crystal surfaces. In contrast, we succeeded in visualizing elementary steps only when a flat terrace was exposed widely (Figure 5). The elementary steps marked by two white triangles in Figure 5I advanced toward the upper-left direction under the supersaturated condition (from -40 to 0 s) and receded toward the lower-right direction under the undersaturated condition (from 0 to 30 s). From the advancement and recession of the elementary steps, we could accurately determine the water vapor pressure at which water vapor and a solid ice were in equilibrium. The vapor-ice (gas-solid) equilibrium pressures thus determined in the presence of HCl gas agree with the vapor-ice equilibrium curve obtained in the absence of HCl gas (Figure 2). Therefore, we concluded that the presence of HCl gas (100 Pa) does not affect the equilibrium between water vapor and a solid ice. This result is supported by the fact that the ice/water distribution coefficient of chloride ions is very small (2.78×10^{-3}).¹⁹

We also paid our attention on the stability of the droplet QLLs. As shown in Figure 5, the droplet QLLs existed on the

ice basal face for 1 h under the undersaturated condition. When the water vapor pressure is lower than the solid–vapor equilibrium curve (Figure 2), thermodynamic stabilities are in the order of water vapor (most stable) > ice > liquid water (least stable). Hence, if the droplet QLLs were bulk pure water, they were least stable: the droplet QLLs of submicron height should be evaporated into water vapor or crystallized into ice. Therefore, the long-term existence of the droplet QLLs on the ice basal face strongly suggests that the droplet QLLs were thermodynamically stable: the droplet QLLs were not bulk pure water.

Physical properties of QLLs are still not fully clarified, and there is plenty of room for argument. Hence, the simplest discussion here would be about conditions under which bulk of the droplet QLLs can become thermodynamically stable. Using previous experimental data,²⁰ we calculated that the solubilities of the 100 Pa HCl gas (initially filled in the chamber) in water at -15.0 to -1.5 °C are over 23 wt % (eutectic point), whose freezing point is -75 °C.²¹ Hence, once we assume that the droplet QLLs were HCl solutions, we can explain the reason why the droplet QLLs did not freeze or evaporate. As HCl concentration of the droplet QLL increases, the freezing point of the HCl solution decreases (below 0 °C). The freezing point of a 10 wt % HCl solution is -15.0 °C,²⁰ which was the lowest temperature of our experiments. Since we could observe the droplet QLL at -15.0 °C (Figure 5), the HCl concentration in the droplet QLL would be ≥ 10 wt %. The competition between the increase in the HCl concentration (by the dissolution of HCl gas and the evaporation of a droplet QLL) and the decrease in the HCl concentration (by the condensation of water vapor and the melting of an ice crystal) probably determined the actual HCl concentration in the droplet QLL. The long-term existence of the droplet QLLs under the undersaturated conditions (Figures 4 and 5) suggests that the melting rate of the ice crystals was equal to or larger than the evaporation rate of the droplet QLLs.

In addition, under the undersaturated conditions, we observed the appearance of the finger-like pattern and the splitting of the droplet QLLs. We suppose that these phenomena are closely related to the evaporation of the droplet QLLs and the subsequent melting of ice crystals caused by the increase in the HCl concentration. We could not observe the appearance of the finger-like pattern and the splitting of the droplet QLLs in the absence of HCl gas. Hence, at present, we have no experimental evidence that implies mechanisms of these phenomena. In this study, we mainly observed the appearance of the droplet QLLs, although the precise observation of melting processes of ice crystals (receding processes of elementary steps) will give us a hint for unlocking such phenomena. We plan to achieve such observation in the near future.

4. CONCLUSIONS

We directly visualized the QLLs on ice basal faces in the presence of the HCl gas using the LCM-DIM system. We found that the HCl gas induced the appearances of the droplet QLLs in the temperature range of -15.0 to -1.5 °C, where no QLL appears in the absence of the HCl gas. This result suggests that HCl gas adsorbed on ice crystal surfaces changed the surface structure of ice crystals and then induced the subsequent melting of ice surfaces. Since the lowest temperature of our experimental setup is -15.0 °C, the lowest temperature for the appearance of the droplet QLLs is still

unknown. When the water vapor was supersaturated and equilibrium, the shape of the droplet QLLs did not change. However, when the water vapor was undersaturated, the droplet QLLs exhibited the finger-like pattern and broke into smaller ones, although the reason is still unclear. The long-term (1 h) existence of the droplet QLLs under the undersaturated conditions strongly suggests that the droplet QLLs were not bulk pure water but a thermodynamically stable phase (most probably a HCl solution). Insights into the behavior of the HCl-induced droplet QLLs obtained in this study may provide a clue to unlocking roles of QLLs in various chemical reactions on ice crystal surfaces.

■ ASSOCIATED CONTENT

S Supporting Information

The Supporting Information is available free of charge on the ACS Publications website at DOI: 10.1021/acs.cgd.6b00044.

Differential interference contrast, interference image of a droplet QLL in the presence of HCl gas, and full captions for Movies S1 and S2 (PDF)

Movie S1: Behavior of droplet QLLs on an ice basal face in the presence of HCl gas during the change from supersaturated to undersaturated condition (MPG)

Movie S2: Behavior of droplet QLLs on an ice basal face in the presence of HCl gas during the increase in the degree of undersaturation of the water vapor (MPG)

■ AUTHOR INFORMATION

Corresponding Author

*E-mail: nagasima@lowtem.hokudai.ac.jp. Phone and fax: +81-11-706-6881.

Present Address

[†]H.A.: Department of Creative Technology Engineering, Anan National College of Technology, 265 Aoki Minobayashi, Anan, Tokushima 774-0017, Japan.

Author Contributions

K.N., G.S., and T.H. designed the research performed by K.N., G.S., and H.A. K.N., G.S., K.M., and Y.F. wrote the paper. The authors declare no conflict of interest. All authors have given approval to the final version of the manuscript.

Funding

This work was partially supported by JSPS KAKENHI Grant Numbers 15H02016 and 25870009.

Notes

The authors declare no competing financial interest.

■ ACKNOWLEDGMENTS

The authors thank Y. Saito and S. Kobayashi (Olympus Engineering Co., Ltd.) for their technical support of LCM-DIM and S. Nakatsubo (Hokkaido University) for production of the experimental system.

■ ABBREVIATIONS

QLL, quasi-liquid layer; HCl, hydrogen chloride; LCM-DIM, laser confocal microscopy combined with differential interference contrast microscopy

■ REFERENCES

- (1) Bartels-Rausch, T. Ten things we need to know about ice and snow. *Nature* 2013, 494, 27–29.

- (2) Kuroda, T.; Lacmann, R. Growth kinetics of ice from the vapour phase and its growth forms. *J. Cryst. Growth* **1982**, *56*, 189–205.
- (3) Dash, J. G.; Rempel, A. W.; Wetzlaufer, J. S. The physics of premelted ice and its geophysical consequences. *Rev. Mod. Phys.* **2006**, *78*, 695–741.
- (4) Faraday, M. *Experimental Researches in Chemistry and Physics*; Taylor & Francis: London, 1859; pp 372–374.
- (5) Sazaki, G.; Zepeda, S.; Nakatsubo, S.; Yokomine, M.; Furukawa, Y. Quasi-liquid layers on ice crystal surfaces are made up of two different phases. *Proc. Natl. Acad. Sci. U. S. A.* **2012**, *109*, 1052–1055.
- (6) Elbaum, M.; Lipson, S. G.; Dash, J. G. Optical study of surface melting on ice. *J. Cryst. Growth* **1993**, *129*, 491–505.
- (7) Petrenko, V. F.; Whitworth, R. W. *Physics of Ice*; Oxford University Press: Oxford, 1999.
- (8) Li, Y.; Somorjai, G. A. Surface premelting of ice. *J. Phys. Chem. C* **2007**, *111*, 9631–9637.
- (9) Sazaki, G.; Matsui, T.; Tsukamoto, K.; Usami, N.; Ujihara, T.; Fujiwara, K.; Nakajima, K. In situ observation of elementary growth steps on the surface of protein crystals by laser confocal microscopy. *J. Cryst. Growth* **2004**, *262*, 536–542.
- (10) Sazaki, G.; Zepeda, S.; Nakatsubo, S.; Yokoyama, E.; Furukawa, Y. Elementary steps at the surface of ice crystals visualized by advanced optical microscopy. *Proc. Natl. Acad. Sci. U. S. A.* **2010**, *107*, 19702–19707.
- (11) Asakawa, H.; Sazaki, G.; Nagashima, K.; Nakatsubo, S.; Furukawa, Y. Prism and other high-index faces of ice crystals exhibit two types of quasi-liquid layers. *Cryst. Growth Des.* **2015**, *15*, 3339–3344.
- (12) Sazaki, G.; Asakawa, H.; Nagashima, K.; Nakatsubo, S.; Furukawa, Y. How do quasi-liquid layers emerge from ice crystal surfaces? *Cryst. Growth Des.* **2013**, *13*, 1761–1766.
- (13) Murata, K.; Asakawa, H.; Nagashima, K.; Furukawa, Y.; Sazaki, G. In situ determination of surface tension-to-shear viscosity ratio for quasiliquid layers on Ice Crystal Surfaces. *Phys. Rev. Lett.* **2015**, *115*, 256103.
- (14) Asakawa, H.; Sazaki, G.; Yokoyama, E.; Nagashima, K.; Nakatsubo, S.; Furukawa, Y. Roles of surface/volume diffusion in the growth kinetics of elementary spiral steps on ice basal faces grown from water vapor. *Cryst. Growth Des.* **2014**, *14*, 3210–3220.
- (15) Wetzlaufer, J. Impurity Effects in the premelting of ice. *Phys. Rev. Lett.* **1999**, *82*, 2516–2519.
- (16) Huthwelker, T.; Ammann, M.; Peter, T. The uptake of acidic gases on ice. *Chem. Rev.* **2006**, *106*, 1375–1444.
- (17) Grannas, M.; Jones, A. E.; Dibb, J.; Ammann, M.; Anastasio, C.; Beine, H. J.; Bergin, M.; Bottenheim, J.; Boxe, C. S.; Carver, G.; Chen, G.; Crawford, J. H.; Domine, F.; Frey, M. M.; Guzman, M. I.; Heard, D. E.; Helmig, D.; Hoffmann, M. R.; Honrath, R. E.; Huey, L. G.; Hutterli, M.; Jacobi, H. W.; Klan, P.; Lefer, B.; McConnell, J.; Plane, J.; Sander, R.; Savarino, J.; Shepson, P. B.; Simpson, W. R.; Sodeau, J. R.; von Glasow, R.; Weller, R.; Wolff, E. W.; Zhu, T. An overview of snow photochemistry: evidence, mechanisms and impacts. *Atmos. Chem. Phys.* **2007**, *7*, 4329–4373.
- (18) McNeill, V. F.; Loerting, T.; Geiger, F. M.; Trout, B. L.; Molina, M. J. Hydrogen chloride-induced surface disordering on ice. *Proc. Natl. Acad. Sci. U. S. A.* **2006**, *103*, 9422–9427.
- (19) Gross, G. W.; Wong, P. M.; Humes, K. Concentration dependent solute redistribution at the ice–water phase boundary. III. Spontaneous convection. Chloride solutions. *J. Chem. Phys.* **1977**, *67*, 5264–5274.
- (20) Fritz, J. J.; Fuget, C. R. Vapor pressure of aqueous hydrogen chloride solutions, 0° to 50°C. *Chem. Eng. Data Ser.* **1956**, *1*, 10–12.
- (21) Martin, S. T. Phase transitions of aqueous atmospheric particles. *Chem. Rev.* **2000**, *100*, 3403–3453.